

# **Catalytic cracking of *n*-alkane naphtha: The impact of olefin addition and active sites differentiation**

Avelino Corma<sup>a,\*</sup>, Jesús Mengual<sup>b</sup>, Pablo J. Miguel<sup>c</sup>

<sup>a</sup>*Instituto de Tecnología Química, UPV-CSIC, Universidad Politécnica de Valencia, Av. de los Naranjos s/n, 46022 Valencia, Spain*

<sup>b</sup>*Instituto Universitario de Investigación de Ingeniería del Agua y Medio Ambiente, IIAMA, Universidad Politécnica de Valencia, Camino de Vera s/n, 46022 Valencia, Spain*

<sup>c</sup>*Departamento de Ingeniería Química, ETSE-UV, Universitat de València, Av. de la Universitat s/n, 46100 Valencia, Spain*

\* Corresponding author. Fax: +34 963877809. E-mail: [acorma@itq.upv.es](mailto:acorma@itq.upv.es) (A. Corma).

## ***ABSTRACT***

An extended dual kinetic model allows to fit the *n*-heptane cracking results working in a wide range of reaction conditions. The duality of the model is provided by the contribution of monomolecular and bimolecular cracking mechanisms. It takes into account the role played by the olefins formed on the global cracking or added within the feed. Furthermore by means of this model and the kinetic parameters obtained when cracking *n*-heptane on ZSM-5, it has been observed that, while some characterization techniques show a homogeneous zeolite surface from the point of view of the active sites, rigorous kinetic experiments point to the possibility that the reactant sees a heterogeneous surface with, at least, two group of cracking active sites. Those differentiated active sites give different cracking rates and different activation energies for the process and, in the case of ZSM-5, could be assimilated to sites pointing to the 10R channels and sites pointing into the crossing of the 10R channels, mainly due to differences in acid site location and confinement effects.

***Keywords***

Catalytic cracking; Cracking mechanisms; Kinetic models; Zeolite ZSM-5;  
Naphtha; Isosteric heat; Differential heat; Temperature-Programmed desorption.

## 1. Introduction

Alkane cracking is one of the most widely used test reactions to investigate cracking activity of zeolites [1 - 3]. It is accepted the cracking of alkanes occurs via two mechanisms, one of them monomolecular and the other bimolecular [4 - 6]. Despite the complexity of the global process, the conversion results are normally fitted to a pseudo-first order kinetic expression [7 - 9]. This is an approximation that becomes acceptable when working in a specific and restricted area of the multivariable space of catalytic cracking. However when the range of study is expanded, the pseudo-first order cracking kinetic model can not explain the experimental results, and a more complex kinetic model is required. Under those situations the mono and the bimolecular cracking mechanism occur simultaneously, and since the two mechanisms are not completely independent, the relative extent at which each one occurs has a direct impact on the final product distribution. In this sense, there are not independent hydrogen transfer reactions in the possible reaction schemes, something which makes difficult the exact determination of the contribution of each cracking mechanism [10, 11]. Until now the contribution of each one of the two cracking mechanism has been established either approximately by considering the selectivities to certain products [12] or, more rigorously, by establishing complete cracking reaction schemes where the elemental reactions that follows a given molecule are specified. [2, 13 - 24]. By model fitting using the product distribution, it is possible to determine the extent for each elemental reaction and the corresponding kinetic parameters. It has to be considered that, while the above kinetic treatment can be easily done for shorter chain hydrocarbons, it becomes more difficult to apply for cracking of longer chains for which the number of possible scissions and reactions with products grow exponentially. Interestingly, the above is not a limitation for using the model here proposed where only the degree of conversion of the feed is considered as the dependent variable.

In the present work a new kinetic model is presented (Extended Dual kinetic model, ED) [25]. The ED model, though it is a simplified model, it has been at the same time rigorously derived and it is able to differentiate and quantify the contribution of mono and bimolecular cracking when both mechanisms occur simultaneously. It can also show if there are two type of sites on the catalyst that crack the feed at different rates and with different activation energies. This model can replace the oversimplified pseudo-first order model being able to fit well the results in a wide range of conditions including the introduction of ofefins within the feed.

The acceptance of the introduced Extended Dual kinetic model for cracking implies the contribution of two different monomolecular cracking ( $M_1$  and  $M_2$ ), with different apparent activation energies. This fact can suggest a heterogeneous catalytic surface with sites of different energies in the zeolite [26]. Under these circumstances a site distribution could be simulated by assuming two groups of centers with different enthalpies of adsorption, that in our case has been modeled by considering the difference in sites pointing to the 10R channels and sites pointing into the crossing of the 10R channels, which will be mainly due to differences in location and confinement effects. Contrary to this hypothesis, some physicochemical characterization techniques suggest an homogeneous distribution of acid sites within the ZSM-5 zeolite [27 - 29]. In those reports, a single value for the adsorption enthalpies of a probe molecule suggested an uniform strength of the sites. For instance, Niwa et al. [30 - 34] have used thermally programmed desorption (TPD) of ammonia and they found a small distribution of ammonia adsorption heat in the case of ZSM-5. Consequently, the authors conclude that an uniform distribution of acid strengths exist [31]. Others have determined the isosteric heat of adsorption ( $q^{st,\theta}$ ), that gives the adsorption heat of a probe molecule at different levels of surface coverage [29, 35 - 38]. Gorte et al. [38 - 41], have obtained for ZSM-5, the isothermal heat of adsorption of bases (by adsorption calorimetry)

with different sizes and basic strengths. Their conclusion is that for each base, the concentration of acid sites in this zeolite structure is equal to the aluminum content and all the sites have the same strength. Lercher et al. [29, 42 - 44], have performed adsorption calorimetry of more representative molecules such as *n*- and *iso*-alkanes with three to nine carbon atoms. For those authors, ZSM-5 appears as an homogeneous surface where the lateral interactions of the molecules with the walls have a big contribution to the adsorption energies observed.

We could conclude from the literature survey that for most of the authors, the acid sites are homogeneous or nearly homogeneous, and it is controlled by the crystal/pore structure independently of the chemical composition.

In the present work, we will validate first the extended dual cracking kinetic model (ED) [25] when olefin is introduced in the feed. Then, from the kinetic parameters obtained we were able to simulate the results that can be expected with the different techniques commonly used to characterize the sites in the zeolite catalysts, showing internal contradictions with some of those characterization techniques when used to evaluate catalytic cracking sites in ZSM-5 zeolite. We will show the existence of active site heterogeneity in the zeolite for cracking alkanes (*n*-heptane) that can be kinetically modeled by considering two groups of sites, which one could be simplify by referring to sites pointing to the 10R channels and sites pointing into the crossing of the 10R channels and that will be different from the point of view of location and confinement effects.

## **2. Experimental**

### *2.1. Reactants and materials*

*n*-Heptane from Aldrich (99+%) was cracked without further purification. Carborundum (Silicon Carbide-CSi granules) was used to dilute the catalyst. A ZSM-5 zeolite sample with a Si/Al ratio of 15 was obtained from Zeolyst (ZSM-5(3020)). Propene (99+%) and He (99.999% purity, used as a carrier gas) were provided by Carburos Metálicos.

## 2.2. Catalyst characterization

Bulk Si/Al ratio of ZSM-5 was determined by chemical analysis, with atomic absorption spectrophotometry (SpectraA-Plus apparatus, Varian). Textural properties were obtained from N<sub>2</sub> adsorption isotherms at 77 K with a Micromeritics ASAP-2000 apparatus after pretreating the sample overnight at 673 K under vacuum. Infrared (IR) experiments (Nicolet 710 FT IR spectrometer) were carried out with wafers of 10 mg cm<sup>-2</sup> thickness, degassed overnight under vacuum at 673 K. Then, pyridine was admitted and, after equilibration, the sample was outgassed for 1 h at increasing temperatures (523 K, 623 K, and 673 K). The spectra were recorded at room temperature before pyridine adsorption and after desorption at different temperatures, being the background subtracted. All spectra were scaled according to sample weight. The characteristics of the [ZSM-5(3020)] sample are given in Table S1.1 (see supplementary material, S1).

## 2.3. Experimental procedure

The experiments at atmospheric pressure were carried out in a continuous fixed bed, quartz reactor of 11 mm internal diameter and 300 mm length, equipped with a coaxial thermocouple for measuring the temperature of the bed. The reactor was heated in an electric furnace. The temperature was varied from 673 up to 973 K. For the catalytic cracking experiments the zeolite was diluted with carborundum and the length of the catalyst bed was kept constant. For the thermal cracking experiments carborundum was used to vary the

volume and therefore the space-time in the reactor. The other operation variables were changed varying the flow of each component and the weight of catalyst and carborundum ( $\tau_v = 0.5 - 6.2$  s,  $\tau_w = 0.75 - 23.2$  kg cat s atm mol<sup>-1</sup>). The flows were measured and controlled with Mass Flow Controllers (Unit Instruments) for gases and with Syringe Pumps (Cole-Parmer 74900 Series, and B. Braun Secura FT) for liquids. The reactor exit was connected to two parallel multisampling, computer controlled, heated valves (0.25 mL loop volume). A hydrocarbon detector is located at the outlet of the valves in order to detect in a very precise way the moment when hydrocarbon fills the first loop. This moment is considered the zero reaction time, and the sample is automatically kept in the first loop. After this, the gases in the loops, for each multisampling, were automatically injected into the G.C. [11]. The components were separated in a 100 m capillary column (Petrocol DH - Supelco) for the first multisampling, and in a 2 m x 1/8" packed column (HayeSep D 80/100) for the second multisampling, and then analyzed using two detectors (FID and TCD), respectively. Several experiments were duplicated and reproducibility was excellent.

### **3. Results and discussion**

#### *3.1. Catalytic experiments.*

##### *3.1.1. Addition of an olefin in the feed to be cracked.*

The Extended Dual kinetic model (ED) [25] given in Eq. (1) describes the catalytic cracking process of alkanes by considering the existence of the mono and bimolecular cracking mechanism and takes into account the presence of olefins during the process, with the corresponding effect on activity (see supplementary material, S2).



$$\tau_w = -\frac{1}{M} \left[ \frac{\varepsilon^2 X_C}{\left(\varepsilon + \frac{B}{M}\right)} + \frac{(1+\varepsilon)^2}{1+\varepsilon + \frac{B}{M}(1+R)} \ln(1-X_C) - \frac{\left(\frac{B}{M}\right)^2 (1-\varepsilon R)^2}{\left(\varepsilon + \frac{B}{M}\right)^2 \left[1+\varepsilon + \frac{B}{M}(1+R)\right]} \ln \left[ 1 + \frac{\left(\varepsilon + \frac{B}{M}\right)}{1 + \frac{B}{M}R} X_C \right] \right] \quad (1)$$

With the objective to revalidate the ED kinetic model, propene has been introduced in the feed together with the alkane to be cracked (*n*-heptane). In Tables S3.1-S3.2 (see supplementary material, S3) the operation conditions and catalytic conversion ( $X_C$ ) have been summarized for the experiments performed at the lowest and highest reaction temperatures studied here (673K and 973K, respectively). In those experiments, the molar fraction of the alkane (paraffin) ( $x_{P_0} = 0.0643$ ) and the molar ratio of propene/alkane (olefin/paraffin) ( $p_{O_0}/p_{P_0} = 0.2$ ) have been kept constant at the reactor inlet. From Eqs. (2-3) it is possible to determine the catalytic conversion degree ( $X_C$ ) by properly considering the thermal contribution [26]. In fact, if the rate constant for thermal cracking ( $k_T$ ) is known, it is then possible to determine the exact value of  $k_C$  (Eq. (2)) and the catalytic conversion degree  $X_C$  (Eq. (3)) without being disguised by the thermal cracking.

$$-\left[\varepsilon X + (1+\varepsilon) \ln(1-X)\right] = k_C \tau_w + k_T \tau_v \quad (2)$$

$$-\left[\varepsilon X_C + (1+\varepsilon) \ln(1-X_C)\right] = k_C \tau_w \quad (3)$$

The kinetic parameters were obtained by fitting the experimental results to Eq. (1), minimizing the sum of the relative error of the weight-time. If the Extended Dual model is able to describe successfully the kinetic behavior, then the kinetic parameters should be similar to those obtained when no olefin was fed. Then, the experimental and theoretical

values for the catalytic conversion versus the weight-time, with and without olefins added in the feed, are presented in Fig. 1 and Fig. S4.1-S4.2 (as well as the pseudo-linearization of the first order (Eq. (3)) (see supplementary material, S4). It can be seen there that the proposed ED kinetic model also reproduces the experiments when propene was introduced together with *n*-heptane. Moreover, the kinetic parameters given in Table 1 are very similar regardless if olefin is fed or not in the experiment. In this table confidence intervals for the kinetic parameters are also included. From the results it can be seen that the differences observed are not statistically significant, confirming the validity of the model and demonstrating the invariance of the model parameters.

It has to be noticed that the pre-exponential factor and activation energy in the Arrhenius equation generally present a strong binary correlation [45]. This also occurs in our case. However, writing the model in an equivalent mathematical form, but with different parameters, can lead to better sums-of-squares surface conditioning (Reparametrization). The new parameters are more readily obtained, but although the correlation between the parameter estimates has been reduced by this reparametrization, the size of the confidence region of the original parameters does not change. We have found that with or without reparametrization the optimum for the fitting is the same, though the parameter estimates present smaller confidence intervals and consequently a smaller binary correlation. In Table 1, the reparametrized preexponential factor values are given, together with the corresponding confidence intervals.

Finally, in Fig. S5.1 (see supplementary material, S5) the Arrhenius plots are given for the experiments at different weight-time, being the fitting very good. It should be noticed however that despite the fact that a good fitting is obtained for a pseudo-first order kinetic model, the fact that the values of the kinetic constants  $k_C$  are higher when propene is cofeed, invalidates the use of the pseudo first order for general application, since this model implies

only a monomolecular cracking mechanism. It is clear, that the introduction of propene in the feed enhances the contribution of the bimolecular cracking that it is not taken into account by pseudo-first order kinetic equation.

### 3.1.2. The bimolecular fraction of catalytic cracking conversion ( $X_b/X_C$ ).

The main products obtained from the cracking of alkanes, either with the mono (m) or the bimolecular (b) cracking mechanism, are olefins (O) and paraffins (P) with a smaller number of carbons than the reactant molecule. In a general way one can represent the reaction as:

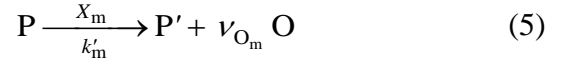


Following the simplified mechanism described, the stoichiometric coefficient of the olefinic fraction ( $\nu_O$ ) in Eq. (4), must have a value  $\geq 1$ . A value higher than one would indicate re cracking of the primary products. Since the nature of the products obtained by either of the two mechanism, i.e. (m) and (b), it is not possible to exactly establish the contribution of each mechanism on the basis of the yields to each product [10]. Wielers et al. [12] have introduced a parameter to describe the relative contribution of each of the two cracking routes, by means of the "cracking mechanism ratio" (CMR). A high value of this index points to a relatively high contribution of the protolytic cracking route, whereas a low value indicates that the classical  $\beta$ -scission route is the main cracking pathway. Nevertheless, the authors conclude that the CMR can be a useful parameter to reveal in a qualitative manner the extent to which the two acid-catalysed cracking mechanisms prevail. On the other hand, the value of the CMR has not a deep mechanistic and quantitative significance since the global cracking mechanism is quite complex. However, it should now be possible by means

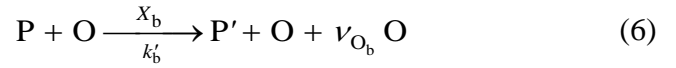
of the ED kinetic model to establish the contribution of the protolytic (monomolecular) and  $\beta$ -scission (bimolecular) on quantitative bases.

Then if one considers the contributions of both mechanisms, i.e. (m) and (b), their separated contribution would be given by:

Monomolecular cracking:



Bimolecular cracking:



where  $\nu_O$ ,  $X$ , and  $k'$ , refer to the stoichiometric coefficient of the olefin, the degree of conversion and the apparent kinetic rate constant for the mono (m) and bimolecular (b) cracking mechanism, respectively.

The development of the corresponding mathematical model (see supplementary material, S6) allows to calculate the change in the degree of conversion due to the monomolecular cracking mechanism as a function of the global degree of conversion. Therefore, knowing the catalytic degree of conversion, it is possible to determine the fraction coming from the mono and from the bimolecular cracking mechanism, and consequently the relative contribution of each mechanism to the total cracking observed (Eqs. (7, 8)):

$$\frac{X_m}{X_C} = \frac{\varepsilon \left( \frac{B}{M} + \varepsilon \right) X_C + \frac{B}{M} (1 - \varepsilon R) \ln \left[ 1 + \frac{\left( \frac{B}{M} + \varepsilon \right) X_C}{\left( 1 + \frac{B}{M} R \right)} \right]}{X_C \left( \frac{B}{M} + \varepsilon \right)^2} \quad (7)$$

$$\frac{X_b}{X_C} = \frac{X_C - X_m}{X_C} = 1 - \frac{X_m}{X_C} \quad (8)$$

The above equations allow to determine the contribution of each mechanism and to study the evolution of those contributions as a function of the catalytic conversion achieved for a set of given kinetic parameters. Following this, the theoretical variations of the  $X_b/X_C$  fraction as a function of the catalytic conversion for the kinetic parameters optimized with the Extended Dual model, using ZSM-5(3020) as catalyst and with or without propene in the feed, are given in Fig. (2). It can be seen there that in both cases, i.e. with or without propene in the feed, an increase of reaction temperature produces a decrease of the fraction  $X_b/X_C$ . This is due to the fact that the B/M ratio decreases because the monomolecular process is favoured with respect to the bimolecular. The behaviour could be expected from previous results reported in the literature [4, 8, 13, 46 - 48], and as a consequence of the different values for the apparent activation energies for both process (see Table 1), also in agreement with the Extended Dual model.

It has to be pointed out that many authors frequently work at  $X_C \leq 20\%$  to ensure that only the monomolecular mechanism is operative, avoiding the kinetic parameters to be disguised by the influence of the bimolecular mechanism. However, from Fig. (2) it becomes apparent that even at low levels of conversion, working at 773 K, the contribution of the bimolecular mechanism to the global conversion is already  $\sim 10\%$  and can be larger at lower cracking temperatures. If that is so, it appears that the kinetic parameters calculated from a pseudo-first order model may not represent the reality of the phenomena.

Finally, it can be observed that, as could be expected, the addition of olefin favors the bimolecular mechanism, being then the  $X_b/X_C$  ratio  $> 0$  even when conversion tends to zero.

### *3.2. Differentiation of active sites.*

### 3.2.1. Isosteric heat of adsorption ( $q^{st,\theta}$ ).

The experimental determination of the adsorption equilibrium by means of the adsorption isotherms obtained at different temperatures, allows to calculate the isosteric heat of adsorption and to study the homogeneity or heterogeneity of the catalytic surface, from its evolution with coverage.

From the Langmuir adsorption isotherm (Eq. (9)) and the van't Hoff equation (Eq. (10)):

$$\theta = \frac{K p_A}{1 + K p_A} \quad (9)$$

$$\left. \frac{\partial \ln K}{\partial T} \right|_{\theta} = \frac{\Delta H}{RT^2} \quad (10)$$

where  $\theta$ ,  $K$ ,  $\Delta H$ , and  $p_A$  are the fractional coverage, Langmuir adsorption equilibrium constant, adsorption enthalpy, and pressure of adsorbate, respectively.

Considering that the variation of the adsorption enthalpy ( $\Delta H$ ) at constant coverage is defined as isosteric heat of adsorption ( $q^{st,\theta}$ ), it is possible to derive the following equation:

$$\left. \frac{\partial \ln p_A}{\partial \left(\frac{1}{T}\right)} \right|_{\theta} = \frac{q^{st,\theta}}{R} \quad (11)$$

Eq. (11) allows to calculate the isosteric heat of adsorption from the adsorption isotherms, by plotting  $\ln p_A$  versus the inverse of the absolute temperature for a constant surface coverage. In agreement with the Eq (11), if no linear relationship are obtained for the adsorption isosteres, this would be an indication of the presence of active sites with clear differences in energy [35].

The coverage of one type of centers assuming the Langmuir adsorption model [49] is given by the following equation:

$$\theta_i = \frac{K_i p_A}{1 + K_i p_A} \quad (12)$$

where  $K_i$  is the Langmuir adsorption equilibrium constant for a  $i$ -type center. Meanwhile the correlation between the equilibrium constant and the temperature involves the changes of enthalpy and entropy of the adsorption process, that result in Eq. (13) when applied to a specific  $i$ -type site.

$$K_i = \exp\left[\frac{\Delta S_i}{R}\right] \exp\left[-\frac{\Delta H_i}{RT}\right] / p^0 = K_i^* \exp\left[-\frac{\Delta H_i}{RT}\right] / p^0 \quad (13)$$

where  $\Delta S_i$  and  $\Delta H_i$  correspond to the change of entropy and enthalpy, respectively, involved in the adsorption process on a  $i$ -site.

In the case of solid catalyst with a homogeneous distribution of active sites, the combination of Eqs. (12) and (13) allows to obtain an equation which represents the adsorption isostere.

$$\ln p_A = \ln\left[\frac{\theta_1}{(1-\theta_1)} \frac{1}{K_1^*}\right] + \frac{\Delta H_1}{R} \frac{1}{T} \quad (14)$$

Plotting  $\ln p_A$  versus the inverse of the temperature obtained from the adsorption isotherm, should give a set of parallel lines (isosteres) for each one of the different fractions of the occupied centers, which will have the same slope, that will be proportional to the adsorption enthalpy of the molecule on the active site. On the contrary in the case of a solid catalyst with a heterogeneous surface, i.e. a surface with various types of active sites, each one of those types will result in a different adsorption enthalpy. Therefore, in this case, one should take into account in the total fraction of sites, the fraction occupied by each one of the types of active sites.

In agreement with the Extended Dual model (see supplementary material, S2) we have considered the possible presence of two groups of different centers that will be named as centers type 1 and type 2. Then, the total fraction of surface coverage will be given by:

$$\theta = \sum_{i=1}^2 x_i \theta_i = x_1 \frac{K_1 p_A}{1 + K_1 p_A} + x_2 \frac{K_2 p_A}{1 + K_2 p_A} \quad (15)$$

where  $x_i$  represents the fraction of  $i$ -type centers.

From Eqs. (11) and (15) the adsorption isosteres and the isosteric heat can be estimated and its evolution with the total fraction of coverage can be studied. It is evident that when two sets of active sites exist, the mathematical representation of the isosteres becomes more complicated than for only one type of sites, as it was given in Eq. (14). Indeed, the equation presented in supplementary material (S7) is quite complex but it can be solved by numerical methods.

It is clear that the estimation of the isosteric heats of adsorption from Eqs. (11) and (15), requires to know the adsorption equilibrium constants as a function of the temperature, as well as the proportion of both types of sites on the catalyst considered. Therefore it will be necessary to use on one hand the information obtained from the kinetic study, where the adsorption parameters are included, and, on the other hand the information found in the literature on the adsorption phenomena.

With respect to the reaction kinetics, the global reaction rate for a catalyst containing two types of active sites acting each one exclusively via monomolecular cracking, can be written as:

$$r_m = k_{m_1} \theta_1 + k_{m_2} \theta_2 \quad (16)$$

It should be pointed out that, despite the fact that we highlight before the importance of considering both mechanisms, i.e. mono and bimolecular cracking to achieve a better kinetic fitting, we want here to discuss the implications of surface heterogeneity for the monomolecular cracking and therefore we will work to do this only under theoretical conditions where the bimolecular cracking is negligible ( $X_C \rightarrow 0$ ). Then if one considers the relationship between the intrinsic kinetic constant per active site ( $k_m^{as} = k_m / D$ ) and  $K_i$  with temperature, for each type of site, and defines a total density of sites  $D_T$ , where:

$$D_i = D_T x_i \quad (17)$$



then it is possible to write, for low surface coverages, the following rate expression:

$$r_m = \left[ A'_{m_1} \exp\left[-\frac{(E'_{m_1})}{RT}\right] + A'_{m_2} \exp\left[-\frac{(E'_{m_2})}{RT}\right] \right] p_A \quad (18)$$

where the different apparent kinetic parameters are given by:

$$A'_{m_1} = A_m^{\text{as}} K_1^* D_T x_1 \quad (19)$$

$$E'_{m_1} = E_m + \Delta H_1 \quad (20)$$

$$A'_{m_2} = A_m^{\text{as}} K_2^* D_T x_2 \quad (21)$$

$$E'_{m_2} = E_m + \Delta H_2 \quad (22)$$

From the Eqs. (19) and (21) one can derive the following relationship:

$$\frac{A'_{m_1}}{A'_{m_2}} = \frac{K_1^* x_1}{K_2^* (1-x_1)} = \frac{K_1^* (1-x_2)}{K_2^* x_2} \quad (23)$$

Since the apparent preexponential parameters ( $A'_{m_1}$  and  $A'_{m_2}$ ) have been obtained experimentally with the Extended Dual kinetic model (Table 1), then Eq. (23) shows the dependence between the entropic factors ( $K_i^*$ ) and the molar fractions ( $x_i$ ) of the existing centers of type  $i$ .

It is possible to find in the literature adsorption entropy and enthalpy values for  $n$ -heptane on the active sites of an H-ZSM-5 zeolite. Following Eder and Lercher [42], the adsorption enthalpy has a value of  $-94.1 \text{ kJ mol}^{-1}$ . In this case the authors consider an homogeneous surface with a unique type of active sites. However, if we consider the results previously presented, an intrinsically better fit is obtained when the possibility that two different sites with different adsorption enthalpies is accepted. Then if one considers the value for the enthalpy of adsorption given by Eder and Lercher [42] as that for the so called sites type 1, and the values for the apparent activation energies for the monomolecular cracking given in Table 1, it is then possible to calculate the value of the intrinsic activation energy

from Eq. (20). By doing that, the intrinsic activation energy obtained is  $192.5 \text{ kJ mol}^{-1}$ , which is in agreement with the values presented by different authors [50 - 52]. Now with the calculated value for the intrinsic activation energy and Eq. (22), it is possible to calculate the adsorption enthalpy for the type 2 cracking sites, being this value  $-147.7 \text{ kJ mol}^{-1}$ , that indicates a stronger adsorption of *n*-heptane on sites type 2 than on sites type 1.

With respect to the adsorption entropy, Eder and Lercher [42] give a value of  $-167.8 \text{ J mol}^{-1} \text{ K}^{-1}$ . In analogy with the above reasoning for the value of adsorption enthalpy, we have assumed that this value of entropy given above should correspond to sites type 1 in the Extended Dual model. Then it is possible to calculate the entropic factor ( $K_i^*$ ) for this type of sites, according to Eq. (13), with the following expression:

$$K_i^* = \exp\left[\frac{\Delta S_i}{R}\right] \quad (24)$$

being the calculated value of  $K_1^*$   $1.71 \cdot 10^{-9}$ . When the value of  $K_1^*$  is known, the value of  $K_2^*$  will depend, following Eq. (23), from the relative amount of type 1 and type 2 sites presents in the catalyst.

We have here evaluated the parameters for two extreme cases: Case I, where the fraction of sites type 1 is 98% and only 2% of sites type 2 are present in the catalysts. This assumption should allow to simulate the situation with a “quasi” homogeneous catalyst. In case II, we have considered that the fraction of sites 1 is 70% and consequently a relatively important 30% of sites type 2 exist on the catalyst.

### 3.2.1.1. Case I, only 2% sites of type 2.

In Table 2 the parameters obtained for the adsorption model corresponding to Case I are given. With these parameters and Eq. (15), it is possible to obtain the adsorption isotherms and isobars for the system: zeolite ZSM-5 as adsorbent and *n*-heptane as adsorbate, and the results are plotted in Fig. (3).

From the adsorption isotherms (Fig. 3A) it can be seen that it is possible to recognize the presence of two different type of sites, if this is enlarged in the range corresponding to coverages ( $\theta$ ) of 0.02, i.e *n*-heptane pressure ranges in the order of  $10^{-6}$  atm. Then, if one could work in that range of pressures, i.e.  $10^{-6}$  atm, it should be possible to observe the effect due to the catalyst heterogeneity (see supplementary material, S8).

In the case of the adsorption isobars (Fig. 3B), to observe the heterogeneity of the catalyst for Case I, it is again necessary to perform the adsorption at very low pressures (see supplementary material, S9). With these values, it is not surprising that under the experimental conditions where the adsorption of hydrocarbons, and more specifically *n*-heptane, have been carried out, the authors have concluded that ZSM-5 has a homogeneous surface from the point of view of the active sites.

From the individual adsorption isobars for each type of center, it can be observed that, being the adsorption constant  $K_1$  lower than  $K_2$ , (in the range of temperatures studied) the latest require a higher temperature for desorbing the reactant (See Fig. 4 and Fig. S10.1). However, it should be remarked that for the temperatures and pressures at which many of the papers on catalytic cracking are reported, the fraction of sites covered can be very small. For instance, if at the inlet of the reactor  $x_{P_0} = 0.0643$ ,  $p_{P_0} = 0.0680$  atm and the reaction temperature is 973 K, the coverage  $\theta$  is  $1.65 \cdot 10^{-5}$ . In other words, only 18 centers are occupied of  $10^6$  possible, being according with the postulate in Case I, 14 sites of type 1 and 4 of type 2. Notice that in an intermediate position along the reactor where the values of conversion are already high, the degree of surface coverage by the *n*-alkane ( $\theta$ ) will present very low values.

However the effect of the heterogeneity, even with only 2% of type 2 sites, becomes much more dramatic when considering their contribution to the final observed activity. Indeed, following Eq. (16) and the  $k_{mi}$  values, the type 2 sites, though being minority are

responsible for 79% of the monomolecular cracking activity observed (88% at 923 K and 99.9 % at 673 K).

After studying the adsorption isotherms and isobars, we will proceed to the determination of the isosteric heats of adsorption and its evolution with site coverage. Since this is a procedure largely used to discuss on the potential heterogeneity of the zeolite surface for different adsorbates, we will proceed here to investigate the experimental conditions required to be able to observe catalyst surface heterogeneity, if present.

The isosteric heat of adsorption, according to Eq. (11), is proportional to the slope of the curve  $\ln p_A$  vs  $1/T$  at constant coverage (adsorption isosteres) [35]. To calculate the values we have worked with the adsorption-desorption equilibrium introduced previously, and for each level of coverage and the corresponding  $p$  and  $T$ , the different isosteres have been generated. The corresponding plots for the equilibrium corresponding to the Case I studied, Figs. 5 and S11.1 (see supplementary material, S11) have been constructed.

The isosteric heat of adsorption for a constant coverage has been obtained from the slope at a given point of one of the above curves, following Eq. (11). It can be seen how the slope of the different curves changes when changing adsorption pressure at constant temperature. This observation indicates the existence of a heterogeneous surface for the adsorbate with a change of the isosteric heat with the surface coverage. Also, for a given curve and at given degree of surface coverage, it can be seen that the value of the slope changes when changing the pressure or the temperature. Since the values of the slope varies, it is of interest to study the limit in the values that can be achieved to discuss the tendencies (see supplementary material, S7.2).

Following Casquero et al. [35] the slope of the curve in the low temperature region tends to the values corresponding to the isosteric heat of the higher energy sites. On the other hand, in the high temperature region the slope comes close to the value corresponding to the

sites with lower energy. However from the derived equations (see supplementary material, S7), in the low temperature region it should be possible to obtain the isosteric heats of adsorption of the sites with higher energy ( $\Delta H_2 = -147.7 \text{ kJ mol}^{-1}$ ) or that of the sites with lower energies ( $\Delta H_1 = -94.1 \text{ kJ mol}^{-1}$ ) for coverages zero and 100%, respectively. In the high temperature region the calculated isosteric heat will depend, not only on the total coverage, but also on the proportion of the different sites and the entropic factor of the adsorption equilibrium constant for both type of centers. We have determined the isosteric heat of adsorption for the high temperature region and the values obtained are  $-94.1 \text{ kJ mol}^{-1}$  and  $-122.2 \text{ kJ mol}^{-1}$  for zero and 100% coverages, respectively.

When one plots the isosteric heat as a function of the total coverage for different temperatures (Fig. 6A), as it is normally done in the literature, it is possible to see how when temperature increases the isosteric heat calculated for coverages below 0.02 progressively decreases. Moreover, for degrees of coverage above 0.02, the isosteric heat (at any temperature) separates rapidly from the value corresponding to the sites with stronger adsorption energy.

Notice that at 1612 K the isosteric heat is constant and does not change with the degree of surface coverage. Of course this is not a realistic temperature for cracking and it is only a virtual situation for which the adsorption equilibrium constant for both types of sites is the same. Such a temperature, named as  $T_{\text{isoK}}$ , can be calculated from Eq. (25). The isosteric heat at this temperature is given by the addition of the adsorption enthalpies of the two types of sites, considering the proportion of each one of those sites in the zeolite (Eq. (26)).

$$T_{\text{isoK}} = \frac{\Delta H_1 - \Delta H_2}{R \ln \left[ \frac{K_1^*}{K_2^*} \right]} \quad (25)$$

$$q_{\text{isoK}}^{st,\theta} = x_1 \Delta H_1 + x_2 \Delta H_2 \quad (26)$$

The isosteric heats of adsorption parameterized for different working pressures are given in Fig. 6B. This type of plot, while being less usual in the literature, can be helpful for better understanding the adsorption process and, in fact, it shows again the surface heterogeneity of the adsorbent since the isosteric heat varies with the degree of coverage. Therefore, Figs. 6A and 6B allow to see that in fact the isosteric heat of adsorption changes with the coverages at different equilibrium temperatures or pressures. Nevertheless it should be taken into account that, following Fig. (5), there is a value of  $\theta$  per each pair of pressure and temperature, which defines a unique isosteric heat.

The mathematical model developed offers the possibility to calculate the isosteric heat of adsorption from the intersection of Figs. 6A and 6B corresponding at a given pressure and temperature, for to the equilibrium coverage ( $\theta$ ). In this way it becomes very simple to predict under what experimental conditions may be possible to see if there is a surface heterogeneity in the catalyst. It is also valuable to know if under a given set of experimental conditions, it is possible to ascertain if the surface of the catalyst is, or it is not, homogeneous. In fact, from the degree of surface coverage and the isosteric heat of adsorptions at given temperatures and pressures of equilibrium given in Figs. 7-8 and Figs. S12-S13 (see supplementary material), we can conclude that when there are only 2% of the most energetic type 2 sites, only by performing the adsorption at  $p < 10^{-6}$  atm and  $T > 453$ K one can ascertain if there is, or there is not, heterogeneity on the adsorption sites in ZSM-5.

### *3.2.1.2. Case II, 30% sites of type 2.*

In this case we have chosen another arbitrary value in the proportion of sites 2 (30%) to see an example with a larger fraction of the most energetic sites. One would think that, a priori, it should be quite easy by the techniques and experimental conditions used up to now in the literature to observe surface heterogeneity by adsorption measurement in a ZSM-5

when would be a population of 70 and 30% of adsorption sites with clear different adsorption energies. However, we will show that this is not the case.

Here, as was done above for Case I, we have analyzed the new situation by taken the same parameters corresponding to sites type 1 and the adsorption enthalpy of sites 2, than in Case I. However,  $K_2^*$  takes a new value according with Eq. (23) since  $x_2$  and  $x_1$  are now different. In Table 2 the values for the parameters of the adsorption-desorption model considered in Case II are given. With the new parameters and following exactly the same methodology than for the previous case, the adsorption isosteres at the different surface coverage have been obtained, and results (see supplementary material, S14) show a similar behavior as for Case I but, as could be expected, with different values. In this second case, with 30% sites 2, the limit values of the isotheric heat calculated for the high temperature range are  $-94.1$  and  $-147.7$   $\text{kJ mol}^{-1}$ , respectively.

As was done before the changes of the isosteric heats *vs.*  $\theta$  have been plotted at different pressures and temperatures in Fig. S15 (see supplementary material, S15). While the qualitative behavior is the same than in Case I, in case II the change in energy at lower temperatures (which marks the difference between the heat of adsorption of both sites), occurs now at a coverage of  $\sim 0.3$ . Moreover, in Case II, the  $T_{\text{isoK}}$  is 915K.

In Fig. (9) and Figs. S16.1-S17.1 (see supplementary material) the degrees of coverage and the isosteric heat at given equilibrium temperature and pressure are shown in an analogous manner as was done for case I. It can be seen that to be able to ascertain the presence or not of heterogeneity by adsorption measurements, it is still necessary to perform the adsorption at pressures  $< 10^{-6}$  atm. Indeed, while it should be possible to perform adsorptions at pressure  $> 10^{-3}$  atm, the required temperature will be then  $> 493$  K, with the corresponding problems associated to potential masking by undesired reactions.

### 3.2.2. Differential heat of adsorption ( $\Delta H_{ads}$ ).

It is clear that the surface heterogeneity of a catalyst for adsorption can also be studied, as commented before, by determining the differential heat of adsorption ( $\Delta H_{ads}$ ). This can be obtained by calorimetric measurements by reversible adsorption of different amounts of adsorbate at constant temperature (isothermal heat of adsorption).

If one considers that there are two energetically differentiated adsorption sites, the heat exchanged in adsorption-desorption process of a given amount of adsorbate on those sites, assuming adsorption of one molecule per site, can be written as:

$$\Delta Q_{ads} = \Delta N_1 \Delta H_1 + \Delta N_2 \Delta H_2 \quad (27)$$

where  $N_i$  represents the number of occupied sites type  $i$ , and  $\Delta H_i$ . their heat of adsorption.

For a very small adsorption of adsorbate, the differential heat of adsorption at constant temperature ( $\Delta H_{ads}$ ) would be given by (see also supplementary material, S18):

$$\Delta H_{ads} = \frac{\Delta H_1}{1 + \left( \frac{1-x_1}{x_1} \right) \frac{d\theta_2}{d\theta_1}} + \frac{\Delta H_2}{1 + \left( \frac{x_1}{1-x_1} \right) \frac{d\theta_1}{d\theta_2}} \quad (28)$$

$$\frac{d\theta_1}{d\theta_2} = \frac{K_1}{K_2} \left[ \frac{(1 + K_2 p_A)}{(1 + K_1 p_A)} \right]^2 \quad (29)$$

By combining Eqs. (28) and (29) is possible to determine theoretically the isothermal adsorption heat of a catalyst at a given temperature and pressure, provided that the thermodynamic parameters of adsorption and the fraction of each type of sites is known. Then, the variation of the isothermal heat of adsorption as a function of the degree of coverage can be studied considering the parameters established for each case (Table 2). The results obtained (see supplementary, S18.2) are practically identical to those from the isosteric



heat and, consequently, the conclusions are equivalent regardless that the experimental procedures for determining the isosteric and isothermal heat of adsorption are based on the adsorption isotherms and direct calorimetric measurements, respectively.

From our results, it appears that most of the adsorption work performed on zeolites to discuss on the homogeneity or heterogeneity of these materials, from the point of view of adsorption sites, may need to be revised. Just as an example, in the work of Eder et al. [29] and De Moor et al. [53], adsorption was carried out at  $p \geq 10^{-3}$  mbar ( $9.87 \cdot 10^{-7}$  atm) of (propane to *n*-hexane) and  $T \leq 400$  K. In an analogous way in the work of Dunne et al. [54], Ramachandran et al. [28] and Ferreira et al. [55], among others, adsorption was always performed at  $p \geq 9.87 \cdot 10^{-5}$  atm and  $T \leq 423$  K. From the work presented here, it is clear that by working under those experimental conditions it should be very difficult to unequivocally conclude about the homogeneity or heterogeneity of the surface for adsorption sites. Then, one should either follow the methodology presented here or to perform adsorption measurements under the appropriate range of pressures and temperatures to ascertain the homo or heterogeneity of the zeolite surface for catalytic cracking.

Therefore, taking into account the ED kinetic model, it is possible the existence of a catalytically heterogeneous ZSM-5 surface, as claimed by some researchers [56 - 60], for catalytic cracking of alkanes and the possibility to identify them in two groups.

### *3.2.3. Temperature-Programmed Desorption (TPD) of ammonia.*

The Temperature-Programmed Desorption (TPD) technique of probe molecules [61, 62] allows, in principle, to study the distribution and characterization of acid sites on solid catalysts. With this technique taking into account the desorption equilibrium and establishing a mass balance in the desorption process, it is possible to model the TPD curves obtained. The

relations found will be a function, among others, of the desorption equilibrium constant, which is itself dependent on the adsorption enthalpy. The TPD has been widely used to characterize solid catalyst and new developments have been made on the methodology [63, 64]. This technique in combination with ammonia has been used with HZSM-5 zeolite to discuss on its acidity [31, 65 - 68]. However, there is still much controversy on the results on homogeneity of the Brønsted acid sites. In fact, some authors claim that the acid sites in HZSM-5 are energetically homogeneous [69 - 71], while others claim the opposite [67, 72 - 73].

Here, in an analogous way as we did before for the isosteric and differential heat of adsorption, we have performed a theoretical simulation of the ammonia TPD on H-ZSM-5 in which readsorption of ammonia occurs freely (adsorption equilibrium) (see supplementary material, S19). Again, and in agreement with the previous discussion, Case I (2% type 2 sites) and Case II (30% type 2 sites) have been considered. The simulation obtained for both cases is given in Fig. (10). It can be seen there, that it would be very difficult, for this catalyst, with a deconvolution process to determine unequivocally surface heterogeneity when there is a small proportion of one of the two different sites. Nevertheless, as we showed above, the presence of a small amount of more energetic sites can be responsible for a very important fraction of the catalytic cracking activity observed.

Therefore, when working under experimental conditions where the monomolecular cracking mechanism is practically exclusively predominant, it is possible to consider, contrary to the conclusion of many adsorption studies, that there are sites in HZSM-5 with different energetics for adsorption and cracking of alkanes (*n*-heptane). Notice that contrary to previous work [27, 51, 75], recent publications are coming to the conclusion that in ZSM-5 there is different acid site reactivity and selectivity as a result of effects of spatial constraints and of

entropic factors [60, 76] or by location at the intersection of straight and sinusoidal channel and within the sinusoidal channel [77].

#### 4. Conclusions

From the results obtained in the present work, the following conclusions can be highlighted:

- A kinetic model named as Extended Dual kinetic model (ED) has been developed. It is able to predict the alkanes cracking results in a wide range of reaction conditions.
- The model can quantify the conversion degree and the extension of the different mono and bimolecular mechanisms when cracking feeds that contain only alkanes and feeds that also contain olefins.
- The ED model is able to show if there is catalyst surface heterogeneity from the cracking reaction point of view.
- Unless adsorption-calorimetric measurements are made in the proper range of experimental conditions, we still need reaction kinetic experiments to determine the presence of one or more type of active sites in cracking catalysts.
- By using the ED model and cracking *n*-heptane on a HZSM-5 catalyst, it appears that the ZSM-5 surface is very probably not homogeneous, from the active site point of view, and acid sites with different energetics for adsorption and cracking of alkanes are present in HZSM-5, mainly due to differences in location and confinement effects.

## **Acknowledgments**

Financial support by the Ministerio de Economía y Competitividad of Spain (MINECO) [Programa Estatal (Project MAT2012-31657) and Programa Consolider-Ingenio 2010 (Project MULTICAT)] is gratefully acknowledged.

## Nomenclature

### Roman Symbols

- $A'_b$  apparent pre-exponential factor for bimolecular cracking [ $\text{mol kg cat}^{-1} \text{s}^{-1} \text{atm}^{-2}$ ]
- $A_m$  pre-exponential factor for monomolecular cracking [ $\text{mol kg cat}^{-1} \text{s}^{-1}$ ]
- $A'_m$  apparent pre-exponential factor for monomolecular cracking [ $\text{mol kg cat}^{-1} \text{s}^{-1} \text{atm}^{-1}$ ]
- $B$  parameter defined as  $B = k'_b p_{P_0} v_O$
- $D_i$  Density of  $i$ th type sites ( $i$ -site  $\text{kg cat}^{-1}$ )
- $E$  activation energy or apparent activation energy [ $\text{kJ mol}^{-1}$ ]
- $F_j$  molar flow rate of  $j$ th component [ $\text{mol s}^{-1}$ ]
- $\Delta H$  adsorption enthalpy [ $\text{kJ mol}^{-1}$ ]
- $\Delta H_{\text{DES}}$  desorption enthalpy [ $\text{kJ mol}^{-1}$ ]
- $\Delta S$  adsorption entropy [ $\text{J mol}^{-1} \text{K}^{-1}$ ]
- $k'_b$  apparent kinetic rate constant for bimolecular cracking [ $\text{mol kg cat}^{-1} \text{s}^{-1} \text{atm}^{-2}$ ]
- $k_C$  global apparent first-order rate constant for catalytic cracking [ $\text{mol kg cat}^{-1} \text{s}^{-1} \text{atm}^{-1}$ ]
- $k_T$  first-order rate constant for thermal cracking [ $\text{s}^{-1}$ ]
- $K_i$  Langmuir equilibrium adsorption constant for  $i$ th type site [ $\text{atm}^{-1}$ ]; Standard pressure  $p^0 = 1 \text{ atm}$ .
- $K_i^*$  parameter defined in Eq. (24)
- $k_m$  intrinsic kinetic rate constant for monomolecular cracking [ $\text{mol s}^{-1} \text{kg cat}^{-1}$ ]
- $k'_m$  apparent kinetic rate constant for monomolecular cracking [ $\text{mol kg cat}^{-1} \text{s}^{-1} \text{atm}^{-1}$ ]
- $M$  parameter defined as  $M = \sum_i k'_{m_i}$
- $N_i$  occupied  $i$ th type sites

O	olefin (alkene)
P	paraffin (alkane)
$p_j$	pressure of jth component [atm]
$q^{st,\theta}$	Isosteric heat of adsorption ( $\text{kJ mol}^{-1}$ )
$Q_{\text{ads}}$	heat exchanged in adsorption-desorption process ( $\text{kJ mol}^{-1}$ )
$R$	universal gas constant [ $\text{kJ K}^{-1} \text{mol}^{-1}$ ]
$R$	parameter defined as $R = \frac{P_{O_0}}{P_{P_0} \nu_O}$
$r$	rate of reaction [ $\text{mol s}^{-1} \text{kg cat}^{-1}$ ]
$T$	absolute temperature [K]
$T_{isoK}$	Temperature defined in Eq. (25)
TPD	Temperature Programmed Desorption
$W$	mass of catalyst [kg]
$X$	overall conversion degree
$X_b$	bimolecular catalytic conversion degree
$X_C$	catalytic conversion degree
$x_j$	mole fraction of jth component
$x_i$	fraction of ith type site
$X_m$	monomolecular catalytic conversion degree
$X_T$	thermal conversion degree

### *Greek Symbols*

$\beta$	ramp rate in TPD experiments [ $\text{K min}^{-1}$ ]
$\nu_j$	stoichiometric coefficient of jth component

$\varepsilon$  volume expansion coefficient (fractional volume change on complete conversion of reactant)

$\theta_i$  fractional of  $i$ th sites coverage

$\tau_v$  space-time for thermal cracking as  $\tau_v = \frac{C_{P_0} V}{F_{P_0}} = \frac{V}{Q_{v_0}}$  [s]

$\tau_w$  weight-time (contact time, modified space-time) for catalytic cracking as

$$\tau_w = \frac{p_{P_0} W}{F_{P_0}} \text{ [kg cat s atm mol}^{-1}\text{]}$$

### *Superscripts*

' apparent

as active site

ch chemisorption

ph physisorption

### *Subscripts*

A adsorbate

A ammonia

b bimolecular

C catalytic

i  $i$ th type site

j  $j$ th component

m monomolecular

O olefin (alkene)

P paraffin (alkane)

rep reparametrized parameter

T thermal

T total



## **Appendix A: Supplementary material**

## References

- [1] J. Abbot, *Appl. Catal.* 57 (1990) 105-125.
- [2] Y. Zhao, G.R. Bamwenda, B.W. Wojciechowski, *J. Catal.* 142 (1993) 465-489.
- [3] G. Yaluris, J.E. Rekoske, R.J. Aparicio, R.J. Madon, J.A. Dumesic, *J. Catal.* 153 (1995) 54-64.
- [4] H. Krannila, W.O. Haag, B.C. Gates, *J. Catal.* 135 (1992) 115-124.
- [5] B.W. Wojciechowski, *Catal. Rev.-Sci. Eng.* 40 (1998) 209-328.
- [6] A. Corma, A.V. Orchillés, *Micro. Meso. Mater.* 35-36 (2000) 21-30.
- [7] D.M. Nace, *Ind. Eng. Chem. Prod. Res. Dev.* 8 (1969) 24-31.
- [8] L. Riekert, J.Q. Zhou, *J. Catal.* 137 (1992) 437-452.
- [9] A. Corma, P.J. Miguel, A.V. Orchillés, *J. Catal.* 145 (1994) 58-64.
- [10] A. Corma, P.J. Miguel, A.V. Orchillés, *J. Catal.* 172 (1997) 355-369.
- [11] A. Corma, P.J. Miguel, A.V. Orchillés, *Ind. Eng. Chem. Res.* 36 (1997) 3400-3415.
- [12] A.F.H. Wielers, M. Vaarkamp, M.F.M. Post, *J. Catal.* 127 (1991) 51-66.
- [13] D.B. Lukyanov, V.I. Shtral, S.N. Khadzhiev, *J. Catal.* 146 (1994) 87-92.
- [14] N. Agarwal, M.A. Sanchez-Castillo, R.D. Cortright, R.J. Madon, J.A. Dumesic, *Ind. Eng. Chem. Res.* 41 (2002) 4016-4027.
- [15] M.A. Sanchez-Castillo, N. Agarwal, A. Bartsch, R.D. Cortright, R.J. Madon, J.A. Dumesic, *J. Catal.*, 218 (2003) 88-103.
- [16] B. de Ménorval, P. Ayrault, N.S. Gnep, M. Guisnet, *J. Catal.*, 230 (2005) 38-51.
- [17] P. Matias, J.M. Lopes, S. Laforge, P. Magnoux, P.A. Russo, M.M.L. Ribeiro Carrott, M. Guisnet, F. Ramôa Ribeiro, *J. Catal.*, 259 (2008) 190-202.
- [18] A.A. Lemonidou, A.P. Koulouris, D.K. Varvarezos, I.A. Vasalos, *Appl. Catal.* 69 (1991) 105-123.

- [19] G.M. Bollas, A.A. Lappas, D.K. Iatridis, I.A. Vasalos, *Catal. Today* 127 (1-4) (2007) 31-43.
- [20] J. Macht, R.T. Carr, E. Iglesia, *J. Am. Chem. Soc.* 131 (2009) 6554-6565.
- [21] W. Knaeble, R.T. Carr, E. Iglesia, *J. Catal.*, 319 (2014) 283-296.
- [22] R. van Borm, M.F. Reyniers, G.B. Marin, *AIChE J.*, 58 (2012) 2202-2215.
- [23] J.W. Thybaut, G.B. Marin, *J. Catal.*, 308 (2013) 352-362.
- [24] M.F. Reyniers, G.B. Marin, *Annu. Rev. Chem. Biomol. Eng.* 5 (2014) 563-594.
- [25] J. Mengual, Doctoral thesis, University of Valencia (2009). *Servei de Publicacions-Universitat de València* (2010). ISBN 978-84-370-7791-8.
- [26] A. Corma, J. Mengual, P.J. Miguel, *Appl. Catal. A: Gen.* 417-418 (2012) 220-235.
- [27] W.O. Haag, R.M. Lago, P.B. Weisz, *Nature* 309 (1984) 589-591.
- [28] C.E. Ramachandran, B.A. Williams, J.A. van Bokhoven, J.T. Miller, *J. Catal.* 233 (2005) 100-108.
- [29] F. Eder, M. Stockenhuber, J.A. Lercher, *J. Phys. Chem. B.* 101 (1997) 5414-5419.
- [30] M. Niwa, N. Katada, M. Sawa, Y. Murakami, *J. Phys. Chem.* 99 (1995) 8812-8816.
- [31] N. Katada, H. Igi, J.H. Kim, M. Niwa, *J. Phys. Chem. B.* 101 (1997) 5969-5977.
- [32] N. Katada, M. Niwa, *Catal Surv. Asia* 8 (2004) 161-170.
- [33] M. Niwa, K. Suzuki, N. Katada, T. Kanougi, T. Atoguchi, *J. Phys. Chem. B.* 109 (2005) 18749-18757.
- [34] M. Niwa, S. Nishikawa, N. Katada, *Micro. Meso. Mater.* 82 (2005) 105-112.
- [35] J.D. Casquero, J.M. Guil, A. Pérez Masiá, A. Ruiz Paniego, *J. Chem. Thermodynamics* 18 (1986) 903-914.
- [36] J.M. Guil, A. Pérez Masiá, A. Ruiz Paniego, J.M. Trejo Menayo, *J. Chem. Thermodynamics* 26 (1994) 5-14.

- [37] A. Corma, A. Chica, J.M. Guil, F.J. Llopis, G. Mabilon, J.A. Perdigón-Melón, S. Valencia, *J. Catal.* 189 (2000) 382-394.
- [38] D.J. Parrillo, R.J. Gorte, *Catalysis Letters* 16 (1992) 17-25.
- [39] D.J. Parrillo, R.J. Gorte, W.E. Farneth, *J. Am. Chem. Soc.* 115 (1993) 12441-12445.
- [40] D.J. Parrillo, C. Lee, R.J. Gorte, *Applied Catal. A.* 110 (1994) 67-74.
- [41] C. Lee, D.J. Parrillo, R.J. Gorte, W.E. Farneth, *J. Am. Chem. Soc.* 118 (1996) 3262-3268.
- [42] F. Eder, J.A. Lercher, *Zeolites* 18 (1997) 75-81.
- [43] F. Eder, J.A. Lercher, *J. Phys. Chem. B.* 101 (1997) 1273-1278.
- [44] F. Eder, J.A. Lercher, *J. Phys. Chem.* 100 (1996) 16460-16462.
- [45] J.R. Kittrell, *Adv. Chem. Eng.* 8 (1970) 97-183.
- [46] W.O. Haag, R.M. Dessau, R.M. Lago, *Stud. Surf. Sci. Catal.* 60 (1991) 255-265.
- [47] X. Wang, H. Carabineiro, F. Lemos, M.A.N.D.A Lemos, F. Ramôa Ribeiro, *J. Mol. Catal. A: Chem.* 216 (2004) 131-137.
- [48] S.M. Babitz, B.A. Williams, J.T. Miller, R.Q. Snurr, W.O. Haag, H.H. Kung, *Appl. Catal. A.* 179 (1999) 71-86.
- [49] I. Langmuir, *J. Am. Chem. Soc.* 40 (1918) 1361-1403.
- [50] T.F. Narbeshuber, H. Vinek, J.A. Lercher, *J. Catal.* 157 (1995) 388-395.
- [51] W.O. Haag, *Stud. Surf. Sci. Catal.* 84 (1994) 1375-1394.
- [52] J.A. van Bokhoven, B.A. Williams, W. Ji, D.C. Koningsberger, H.H. Kung, J.T. Miller, *J. Catal.* 224 (2004) 50-59.
- [53] B.A. De Moor, M.F. Reyniers, O.C. Gobin, J.A. Lercher, G.B. Marin, *J. Phys. Chem. C.* 115 (2011) 1204-1219.
- [54] J.A. Dunne, R. Mariwala, M. Rao, S. Sircar, R.J. Gorte, A.L. Myers, *Langmuir* 12 (1996) 5888-5895.

- [55] A.F.P. Ferreira, M.C. Mittelmeijer-Hazeleger, J. v.d. Bergh, S. Aguado, J.C. Jansen, G. Rothenberg, A.E. Rodrigues, F. Kapteijn, *Micro. Meso. Mater.* 170 (2013) 26-35.
- [56] C. Costa, I.P. Dzikh, J.M. Lopes, F. Lemos, F. Ramôa Ribeiro, *J. Mol. Catal. A: Chem.* 154 (2000) 193-201.
- [57] F. Gaillard, M. Abdat, J.P. Joly, A. Perrard, *Appl. Surf. Sci.* 238 (2004) 91-96.
- [58] P. Borges, R. Ramos Pinto, M.A.N.D.A Lemos, F. Lemos, J.C. Védrine, E.G. Derouane, F. Ramôa Ribeiro, *J. Mol. Catal. A: Chem.* 229 (2005) 127-135.
- [59] G. Caeiro, P. Magnoux, J.M. Lopes, F. Ramôa Ribeiro, S.M.C. Menezes, A.F. Costa, H.S. Cerqueira, *Appl. Catal. A: Gen.* 314 (2006) 160-171.
- [60] R. Gounder, E. Iglesia, *J. Am. Chem. Soc.* 131 (2009) 1958-1971.
- [61] R.J. Cvetanovic, Y. Amenomiya, *Adv. Catal.* 17 (1967) 103-149.
- [62] R.J. Cvetanovic, Y. Amenomiya, *Catal. Rev.* 6(1) (1972) 21-48.
- [63] S. Bhatia, J. Beltramini, D.D., Do, *Catal. Today* 7(3) (1990) 309-438.
- [64] M. Niwa, N. Katada, *Chem. Rec.* 13(5) (2013) 432-455.
- [65] C.V Hidalgo, H. Itoh, T. Hattori, M. Niwa, Y. Murakami, *J. Catal.* 85 (1984) 362-369.
- [66] L. Forni, F.P. Vatti, E. Ortoleva, *Microporous Mater.* 3 (1995) 367-375.
- [67] B. Hunger, M. Heuchel, L.A. Clark, R.Q. Snurr, *J. Phys. Chem. B.* 106 (2002) 3882-3889.
- [68] L. Rodríguez-González, F. Hermes, M. Bertmer, E. Rodríguez-Castellón, A. Jiménez-López, U. Simon, *Appl. Catal. A.* 328 (2007) 174-182.
- [69] F. Lónyi, J. Valyon, *Microporous Mater.* 47 (2001) 293-301.
- [70] K. Suzuki, T. Noda, N. Katada, M. Niwa, *J. Catal.* 250 (2007) 151-160.
- [71] S. Kouva, J. Kanervo, F. Schüßler, R. Olindo, J.A. Lercher, O. Krause, *Chem. Eng. Sci.* 89 (2013) 40-48.
- [72] J. Datka, B. Gil, *J. Mol. Struct.* 596 (2001) 41-45.

- [73] T. Masuda, Y. Fujikata, S.R. Mukai, K. Hashimoto, *Appl. Catal. A.* 165 (1997) 57-72.
- [74] R. Ramos Pinto, P. Borges, M.A.N.D.A Lemos, F. Lemos, J.C. Védrine, E.G. Derouane, F. Ramôa Ribeiro, *Appl. Catal. A.* 284 (2005) 39-46.
- [75] D.H. Olson, W.O. Haag, R.M. Lago, *J. Catal.* 61 (1980) 390-396.
- [76] R. Gounder, E. Iglesia, *Chem. Commun.* 49 (2013) 3491-3509.
- [77] S.M. Sharada, P.M. Zimmerman, A.T. Bell, M. Head-Gordon, *J. Phys. Chem. C.* 117 (2013) 12600-12611.